

Supporting Information for

**Accounting for Changes in Radiation Improves the Ability of SIF to Track Water Stress-Induced Losses in Summer GPP in a Temperate Deciduous Forest**

Zachary Butterfield<sup>1</sup>, Troy Magney<sup>2</sup>, Katja Grossmann<sup>3</sup>, Gil Boher<sup>4</sup>, Chris Vogel<sup>5</sup>,  
Stephen Barr<sup>1</sup>, Gretchen Keppel-Aleks<sup>1</sup>

<sup>1</sup>Climate and Space Sciences and Engineering, University of Michigan, Ann Arbor, Michigan

<sup>2</sup>Department of Plant Sciences, University of California, Davis, California

<sup>3</sup>Institute of Environmental Physics, University of Heidelberg, Heidelberg, German

<sup>4</sup>Civil, Environmental and Geodetic Engineering, Ohio State University, Columbus, Ohio

<sup>5</sup>University of Michigan Biological Station, Pellston, Michigan

**Contents of this file**

Text S1

Figures S1 to S6

**Introduction**

The supporting information include additional methods and results that are relevant but not critical to the conclusions of the paper. Contents include:

- a brief explanation and list of equations used to calculate vegetation indices included in the study;
- several figures that present supplemental information using similar methods as described in the main manuscript.

## Text S1. Equations for calculating vegetation indices

The normalized difference vegetation index (NDVI; Tucker, 1979), photochemical reflectance index (PRI; Gamon et al., 1992), and chlorophyll index (Chlorophyll<sub>RS</sub>; Datt, 1999; Magney et al., 2019) were calculated using the below equations using canopy reflectance observed by the broadband Flame spectrometer (Ocean Optics Inc.).  $R_\lambda$  represents the reflectance at a wavelength of  $\lambda$  nm, or in the red (620-670 nm) or near-infrared (NIR; 830-860 nm) regions of the electromagnetic spectrum.

$$\text{NDVI} = (R_{\text{NIR}} - R_{\text{Red}})/(R_{\text{NIR}} + R_{\text{Red}}) \quad (\text{S1})$$

$$\text{PRI} = (R_{531} - R_{570})/(R_{531} + R_{570}) \quad (\text{S2})$$

$$\text{Chlorophyll}_{\text{RS}} = (R_{850} - R_{710})/(R_{850} + R_{680}) \quad (\text{S3})$$

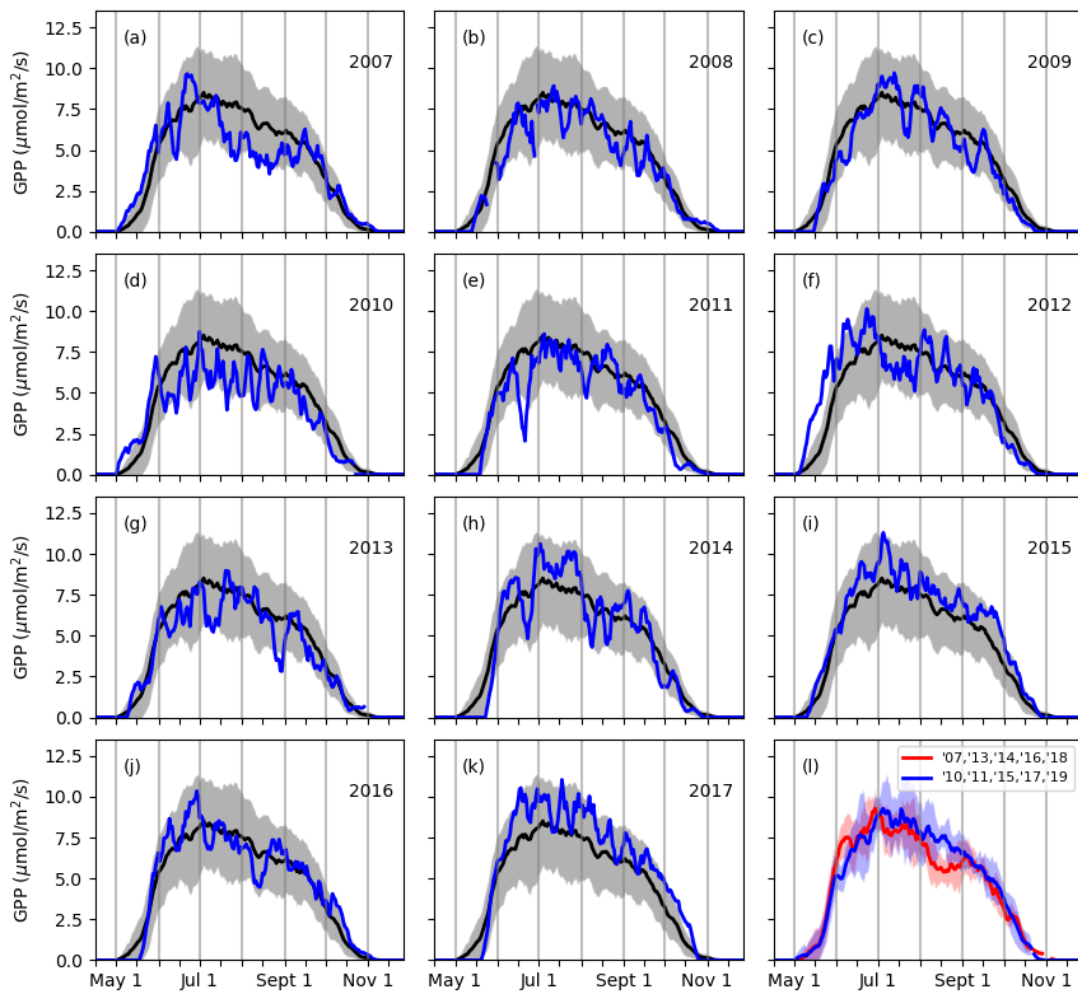


**Figure S1.** Observations of gross primary productivity (GPP) at US-UMB for 2007-2017 (a-k) and composite means of years with and without late-summer dips in productivity (l). In panel l, the mean of 2007, 2013, 2014, 2016, and 2018 is shown in red as years experiencing summer losses in productivity, while the mean of 2010, 2011, 2015, 2017, and 2019 is shown in blue as years that did not see summer losses (see also Figure 1a). The black line in panels a-k represents the 2007-2019 multi-year mean. Shading in all panels represents  $\pm 1$  standard deviation of the respective multi-year means.

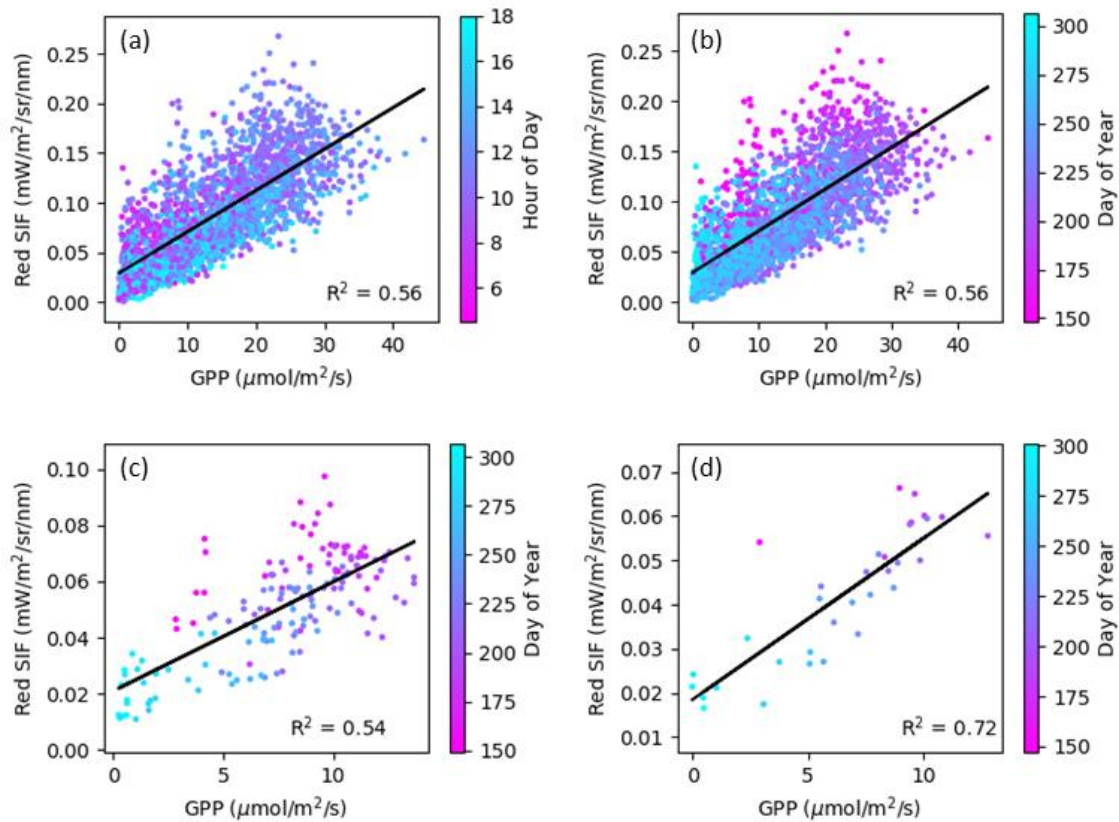


**Figure S2.** Correlation plots between red solar-induced chlorophyll fluorescence (SIF) and GPP at 90-minute (a, b), daily (c), and weekly (d) temporal resolution observations. Color bars are weighted by day of year (b-d) or by hour of day (a).

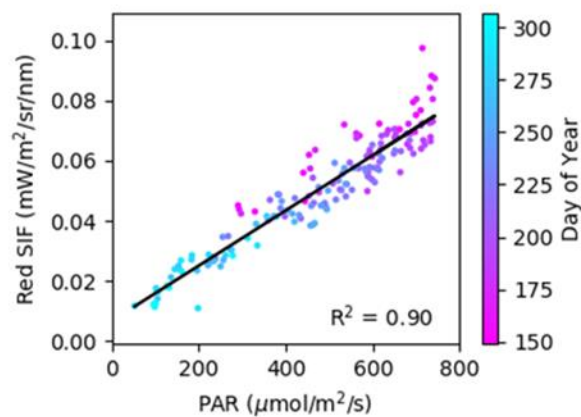


**Figure S3.** Correlation plot between daily-averaged red SIF and photosynthetically active radiation (PAR). Color bar is weighted by day of year.

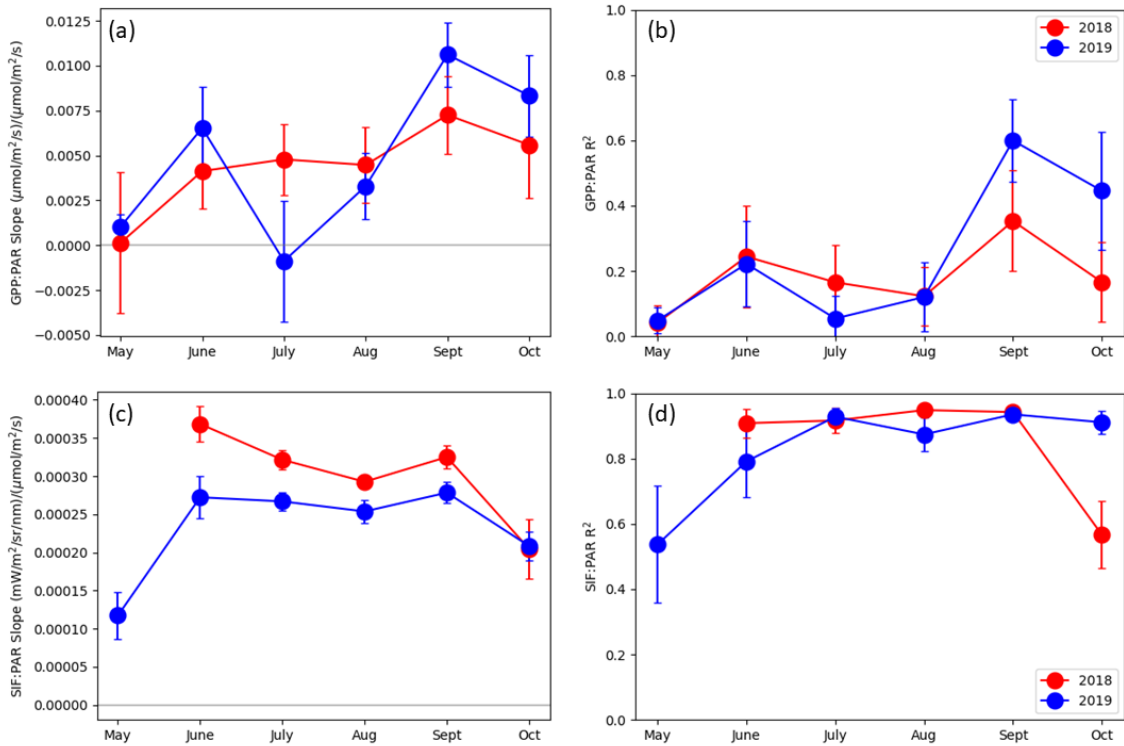


**Figure S4.** Slopes and correlation coefficients from monthly linear fits of daily-averaged GPP (a, b) and far-red SIF (c, d) with PAR. Data from 2018 are in red, while 2019 data are in blue. Error bars represent the standard deviations of results from a bootstrapping method used to test the robustness of the linear regressions.

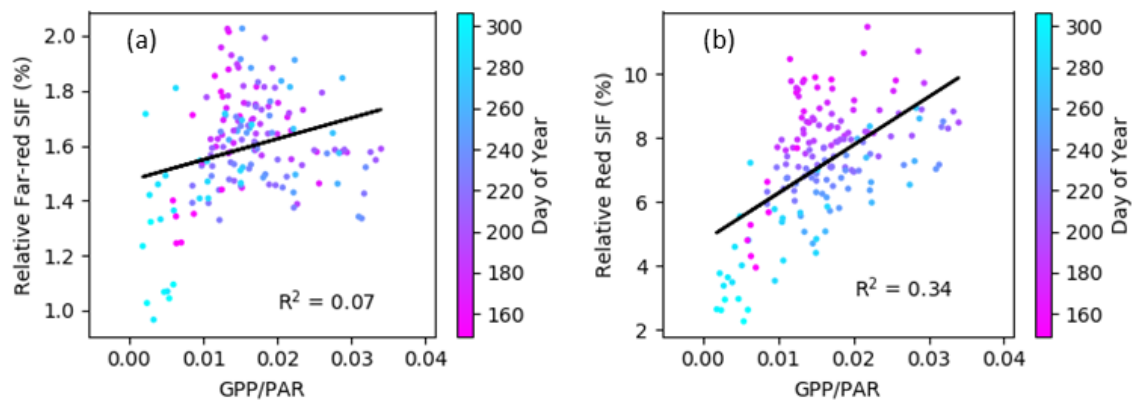


**Figure S5.** Correlation plot between daily-averaged relative far-red (a) and red (b) SIF and GPP/PAR, an LUE proxy. Color bar is weighted by day of year.

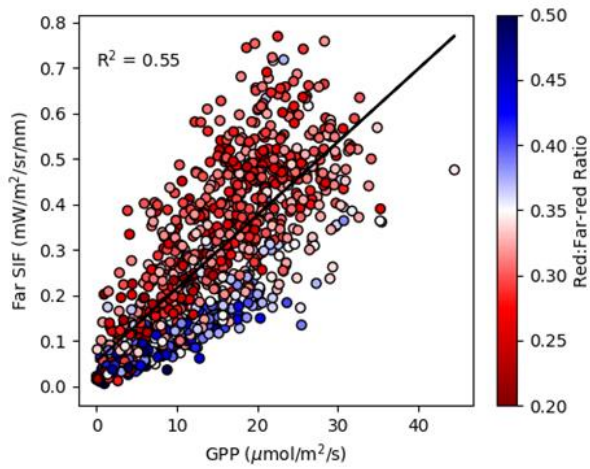


**Figure S6.** Correlation plot between 90-minute far-red SIF and GPP observations. Color scale is weighted by the red:far-red SIF ratio. (Compare with Figure 7b from Magney et al., 2019.)

## References

- Datt, B. (1999). A new reflectance index for remote sensing of chlorophyll content in higher plants: tests using Eucalyptus leaves. *Journal of Plant Physiology*, 154(1), 30–36.
- Gamon, J. A., Penuelas, J., & Field, C. B. (1992). A narrow-waveband spectral index that tracks diurnal changes in photosynthetic efficiency. *Remote Sensing of Environment*, 41(1), 35–44.
- Magney, T. S., Frankenberg, C., Köhler, P., North, G., Davis, T. S., Dold, C., Dutta, D., Fisher, J. B., Grossmann, K., & Harrington, A. (2019). Disentangling changes in the spectral shape of chlorophyll fluorescence: Implications for remote sensing of photosynthesis. *Journal of Geophysical Research: Biogeosciences*, 124(6), 1491–1507.
- Tucker, C. J. (1979). Red and photographic infrared linear combinations for monitoring vegetation. *Remote Sensing of Environment*, 8(2), 127–150.  
[https://doi.org/https://doi.org/10.1016/0034-4257\(79\)90013-0](https://doi.org/10.1016/0034-4257(79)90013-0)